

Heat Transfer Experiments of a 1st Stage Blade Cascade for Supercritical CO₂ Oxy-Combustion Turbine Application

Michael Marshall
Senior Research Engineer
Southwest Research Institute
San Antonio, TX

Mark Anguiano
Research Engineer
Southwest Research Institute
San Antonio, TX

J. Jeffrey Moore, Ph.D.
Institute Engineer
Southwest Research Institute
San Antonio, TX

Noah McElwey
Engineer
Southwest Research Institute
San Antonio, TX



Michael Marshall is a Senior Research Engineer in the Machinery Department at Southwest Research Institute, where he has conducted work on a range of sCO₂ power cycle applications. He earned his Bachelors in Aerospace Engineering in 2018 from the University of Virginia. His past experience includes experimental heat transfer testing, turbomachine and heat exchanger design, root cause failure analysis, and thermodynamic cycle modeling.



Mark Anguiano is a Research Engineer in the Machinery Department at Southwest Research Institute. His research experience includes the design and testing of components such as dry gas seals and cryogenic pumps. He has also designed test loops and ancillary systems (lube oil, dry gas seal) for turbine and compressor powertrains. Mr. Anguiano earned his Bachelor of Science degree and Master of Science Degree in Mechanical Engineering from the University of Texas at San Antonio.



Dr. Jeffrey Moore is an Institute Engineer in the Machinery Section at Southwest Research Institute in San Antonio, TX. He holds a B.S., M.S., and Ph.D. in Mechanical Engineering from Texas A&M University. His professional experience over the last 30 years includes engineering and management responsibilities related to centrifugal compressors and gas turbines at Solar Turbines Inc. in San Diego, CA, Dresser-Rand (now Siemens Energy) in Olean, NY, and Southwest Research Institute in San Antonio, TX. His interests include advanced power cycles and compression methods, rotordynamics, seals and bearings, computational fluid dynamics, finite element analysis, machine design, controls, aerodynamics, and oxy-combustion. He has authored over 40 technical papers related to turbomachinery and has four patents issued. Dr. Moore has held positions as the Vanguard Chair of the Structures and Dynamics Committee and Chair of Oil and Gas Committee for IGTI Turbo Expo. He has also served as the Associate Editor for the Journal of Tribology and a member of the IGTI sCO₂ Committee, Turbomachinery Symposium Advisory Committee, the IFToMM International Rotordynamics Conference Committee, and the API 616 and 684 Task Forces.



Noah McElwey is an Engineer in the Machinery Department at Southwest Research Institute. His work includes designing and building test loops for the thermal cycling of additively manufactured flow components and loop design around various power cycle machinery such as high temp heaters and compressors. He has also designed other ancillary systems (lube oil, flare, steam generators) for various power and refinery machinery. He earned his Bachelors in Mechanical Engineering from Texas A&M University in 2024.

ABSTRACT

The results of internally cooled 1st stage blade (S1B) cascade testing in a supercritical CO₂ environment is presented. The turbine blade design has been previously established for the end application of an oxy-combustion turbine operating in the Allam-Fetvedt cycle with turbine inlet conditions of 305 bar and 1150°C. The internally cooled blade features leading edge (LE) region impingement cooling, mid-section ribbed serpentine passages, and a pin-finned trailing edge (TE) region before cooling ejection holes. The geometry for the tested blade cascade has a cooled central blade with un-cooled blades on either side to match flowpath areas of the actual turbine. The flowpath reuses internal components previously employed for mid-section region ribbed serpentine passage experiments that established Nusselt number enhancement ratios over a range of Reynolds numbers from 100,000-400,000. New components include flow conditioning plates upstream and downstream of the blade cascade to adequately represent the flow field and blade external heat transfer coefficient profiles for the actual turbine. The cooled central blade utilizes uniform crystal temperature sensors (UCTS) with six sensors each on the blade pressure and suction surfaces distributed radially and from LE to TE. The post-processed UCTS quantified the maximum wall temperature seen at each installed sensor location. The test procedure consisted of establishing supercritical CO₂ cooling flow temperature and flow rate and maintaining it throughout the test. The flow rate aims to match that for the actual in-service turbine blade design and is maintained through an orifice restriction to keep the pressure differential between internal cooling flow and external hot flow nearly constant. For the sCO₂ flow path external to the blade, temperatures were ramped throughout the test via control of the test loop's natural gas burner heater. The maximum temperature seen was 468°C and held constant for a duration of 10 minutes at which the blade metal temperature was predicted to be at its maximum before ramping down. For the turbine blade design for service inlet conditions, external flow path computational fluid dynamics (CFD) results and an internal cooling 1-D thermal and hydraulic flow network model using experimentally validated correlations served as thermal finite element (FE) boundary conditions to predict blade metal temperatures. These predicted temperatures were subsequently utilized in a structural FE model to predict blade life ratings dictated by Haynes 282 creep strength data, having a strong dependence on temperature. The boundary conditions experienced during testing are used in the same workflow and compared to the experimental results, with the goal of validating the analysis methodology and providing insight on the uncertainty in local metal temperature predictions.

INTRODUCTION

A utility-scale, direct-fired supercritical CO₂ (sCO₂) turbine was designed for operation in the Allam-Fetvedt cycle [1] as part of U.S. Department of Energy (DOE) supported work. The turbine is purposed to utilize coal-derived syngas and the ability to co-fire with natural gas. Key advantages of the direct-fired sCO₂ power cycle are its near zero emissions and compact machinery with the high fluid density; these features form its target as a commercial product to be competitive with a natural gas combined cycle (NGCC) with carbon capture in system efficiency and capital cost. At a scale of 300 MWe, the turbine has a turbine inlet temperature of 1150°C and an inlet pressure of 305 bar. The design process encompassed pressure containment, thermal and mechanical design, and the turbine's rotordynamics and sealing systems [2]. The predicted thermodynamic efficiency of the turbine is 92% with a per unit cost of \$96/kWe.

The design of the 1st stage blade (S1B) was the culmination of an analysis process incorporating aerodynamic optimization and thermal and structural finite element (FE) evaluation with supporting materials and heat transfer testing. The aerodynamic optimization process sought to

maximize isentropic efficiency and minimize its heat load by varying blade profile 3D geometric parameters [3]. CFD simulations, leveraging an unsteady Reynolds Averaged Navier Stokes (URANS) solver, were able to predict external heat loading characteristics incorporating the effects of platform cooling between the stage 1 nozzle (S1N) and S1B. Thermal barrier coating (TBC) thermal cyclic testing was conducted for Haynes 230 coupons with a MCrAlY bond coat and thermal sprayed (YSZ) top coat; this testing led to a target TBC temperature of 1050°C where degradation was witnessed to be minimal during testing. Due to the significantly higher Reynolds number of CO₂ compared to the use of air as a coolant in an air-breathing engine, focused testing was completed for internal cooling design features of leading edge impingement [4], mid-section ribbed serpentine channels [5], and trailing edge pin-fin array [6]. These test campaigns allowed for validation of existing Nusselt number correlations or the enumeration of previously unknown enhancement ratios to the Nusselt number. For the thermal FE analysis, source temperatures and heat transfer coefficients (HTC) were imported from the URANS CFD simulations and blade internal HTCs and source temperatures were input from a 1-D thermal and hydraulic network. The resulting predicted temperature profile of the S1B at turbine design conditions can be seen in Figure 1 as originally published and further described in 2025 [2].

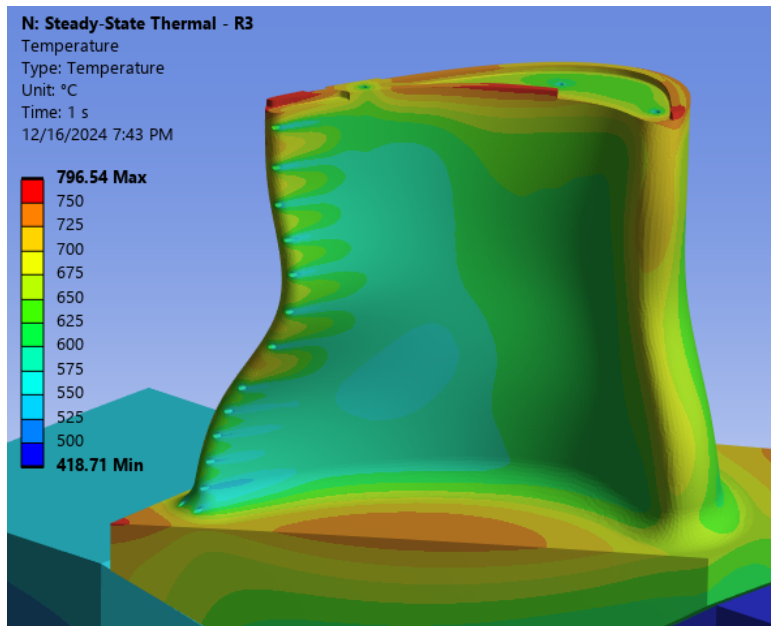


Figure 1. S1B predicted metal temperature profile at full turbine conditions (TIT 1150°C, inlet pressure of 305 bar) [2].

The predicted metal temperatures have a significant influence on blade life ratings due to the metal's (Haynes 282 [7]) creep strength temperature dependence. While the relationship can be best described using the Larson-Miller parameter, an example is the 1000 hr. creep rupture strength decreasing from 262 to 83 MPa from a temperature of 760 to 871°C, respectively. Due to this relationship, it is vital to understand the uncertainties inherent in the temperature profile prediction. One of the main anticipated sources of uncertainty is the localized inaccuracy that may result when using a 1-D thermal and hydraulic network to apply heat transfer coefficient boundary conditions even if those correlations have been experimentally validated. To better enumerate these uncertainties, testing has been completed on a stationary S1B cascade at relevant supercritical CO₂ conditions at comparatively lower temperature. The blade instrumentation technique of uniform crystal temperature sensors (UCTS) was implemented to measure maximum temperatures at different blade locations for comparison to the same

analysis methodology at test boundary conditions.

SYSTEM DESIGN AND BLADE CASCADE

The test loop utilized the same components as previous testing with mid-section ribbed serpentine channels [5]. Driving flow in the loop is a two-stage sCO₂ centrifugal compressor. A natural-gas fired primary heater is implemented for heat addition to the loop, which also features a printed circuit (PCHE) recuperator. Utilizing flow streams at the heater exit, compressor discharge, and recuperator outlet allow for three different temperatures for the hot external blade flow, blade internal cooling flow, and downstream quench flow respectively. A P&ID for the key flow streams for the test section can be seen in Figure 2, and the physical orientation of these flow streams with typical test conditions in Figure 3.

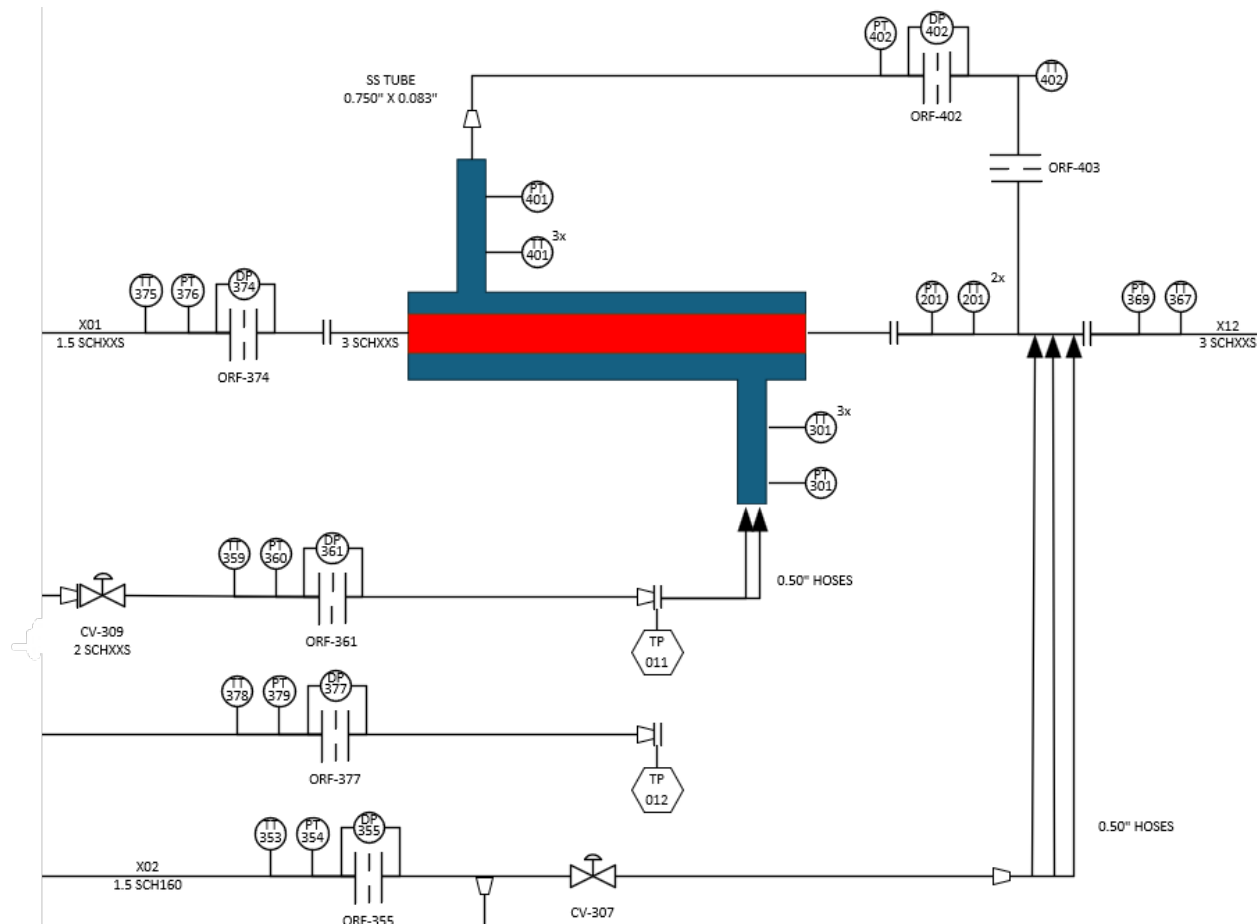


Figure 2. P&ID for test section.

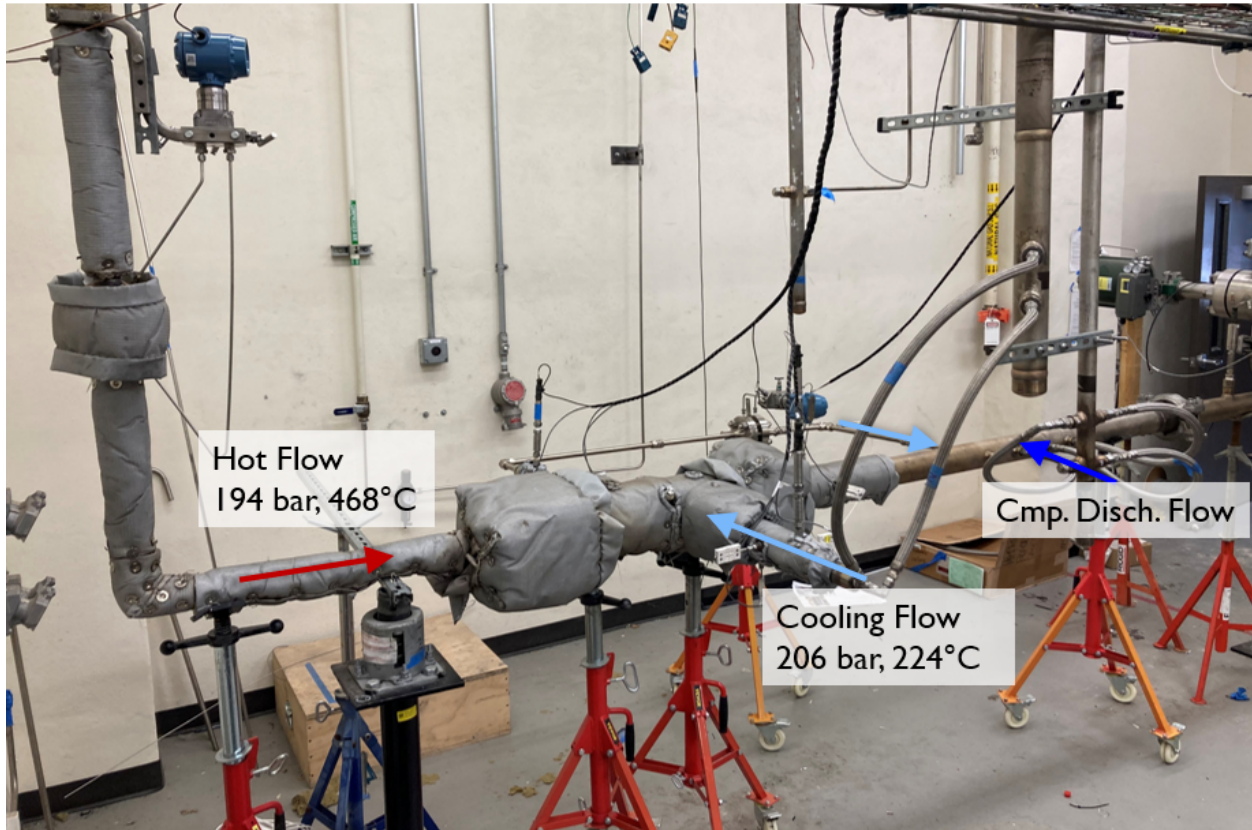


Figure 3. Physical orientation of hot external blade cascade flow, cooling internal blade flow, and compressor discharge quench flow with reference test conditions. All streams are sCO₂ composition.

The main changes made in supporting equipment and instrumentation are the addition of an orifice flow meter (ORF-402) to attempt to measure the differential mass flow from the upstream orifice flow meter (ORF-361) to calculate the blade cooling flow. Additionally, a restriction orifice (ORF-403) was added to generate the required pressure differential (15 bar) between the blade internal cooling flow and external hot sCO₂ path for driving flow internally through blade.

The blade cascade was designed to have a central blade that is an exact replica of the designed S1B with all internal cooling features, and neighboring modified blades without internal cooling for the purpose of providing a relevant flow field around the central blade. For a scale reference, the blade is 1.11 in. in height from platform to tip. The design was specifically tailored to reuse components from the preceding test campaign including the main casing rated for 250 bar and 537°C. The blade was additionally manufactured using a powder bed fusion process with available Inconel 718 powder on hand. Post-processing steps included heat treatment, grinding external blade surfaces to reduce surface roughness, and electrical discharge machining of the blade root mating surfaces. The blade cascade was mated to upstream and downstream flow conditioning plates; the upstream plate served to provide the appropriate flow angle simulating an upstream nozzle and the downstream plate served to prevent flow separation with swirl brake like features. The design of these plates was informed by CFD simulations of the test setup comparing the relative external heat profile to the URANS CFD simulations for the actual stage design, and observing streamlines to ensure no major flow separation was predicted.

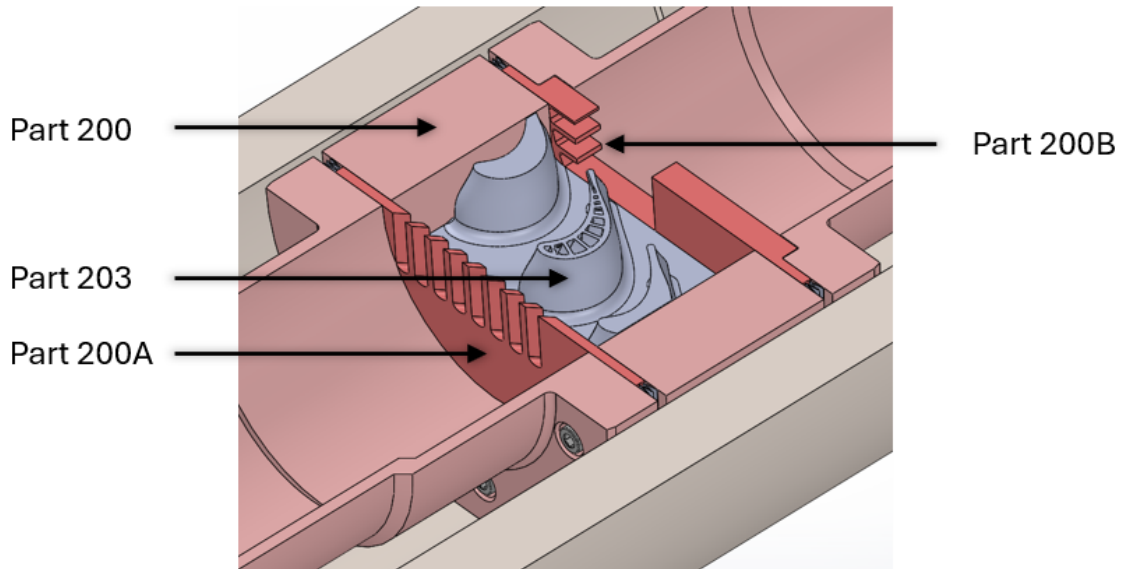


Figure 4. Cross-section of test section internal flowpath with blade cascade (Part 203), upstream flow conditioning plate (Part 200A), downstream flow conditioning plate (Part 200B), and main insert that mates with blade root (Part 200).

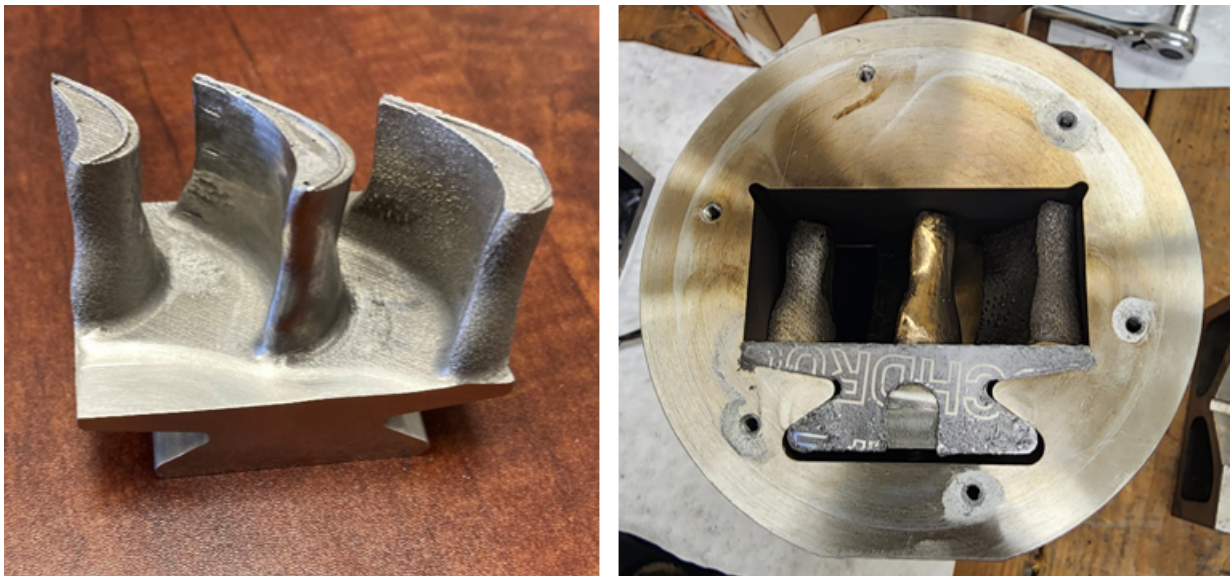


Figure 5. Left: Modified blade cascade after its additive manufacturing and post-processing; Right: Disassembly post-test showing mating surfaces of blade cascade and main insert.

UCTS were installed by LG-Tech Link Global at six locations on the pressure-surface and six locations on the suction-surface. The SiC crystals are embedded in the blade outer wall with an installation process specialized for low wall thickness and the ability to handle harsh turbine environments. The SiC are given dislocations, which anneal during testing as a function of the exposure temperature and time duration. Through post-processing the changes in crystal lattice structure, the max temperature seen at each crystal can be extracted [8]. The UCTS process has been used and improved over more than a decade with successful uses in a range of turbine conditions for accurate temperature measurement [9,10].

TEST OPERATION AND DATA REDUCTION

For the test, the main objectives were to reach a maximum blade temperature condition for a stable period on the order of 10 minutes while keeping blade cooling flow rates and conditions nearly constant. These criteria had dual purposes of providing a temperature history conducive to the post-processing techniques of the UCTS and matching the internal cooling flow for the actual S1B target design conditions. After initial compressor startup, the primary heater fuel flow was increased to raise the hot external blade flowpath temperature. Control valves downstream of the test section and downstream of the recuperator outlet were used to manipulate the respective flow rates of the hot flow and cooling flow; the implementation of the restriction orifice helped stabilize the flow rate ejecting through the blade. The temperature history for the hot external blade flow and blade internal cooling flow can be seen in Figure 6; the pressure history for the blade cooling supply flow and hot external blade flow outlet can be seen in Figure 7.

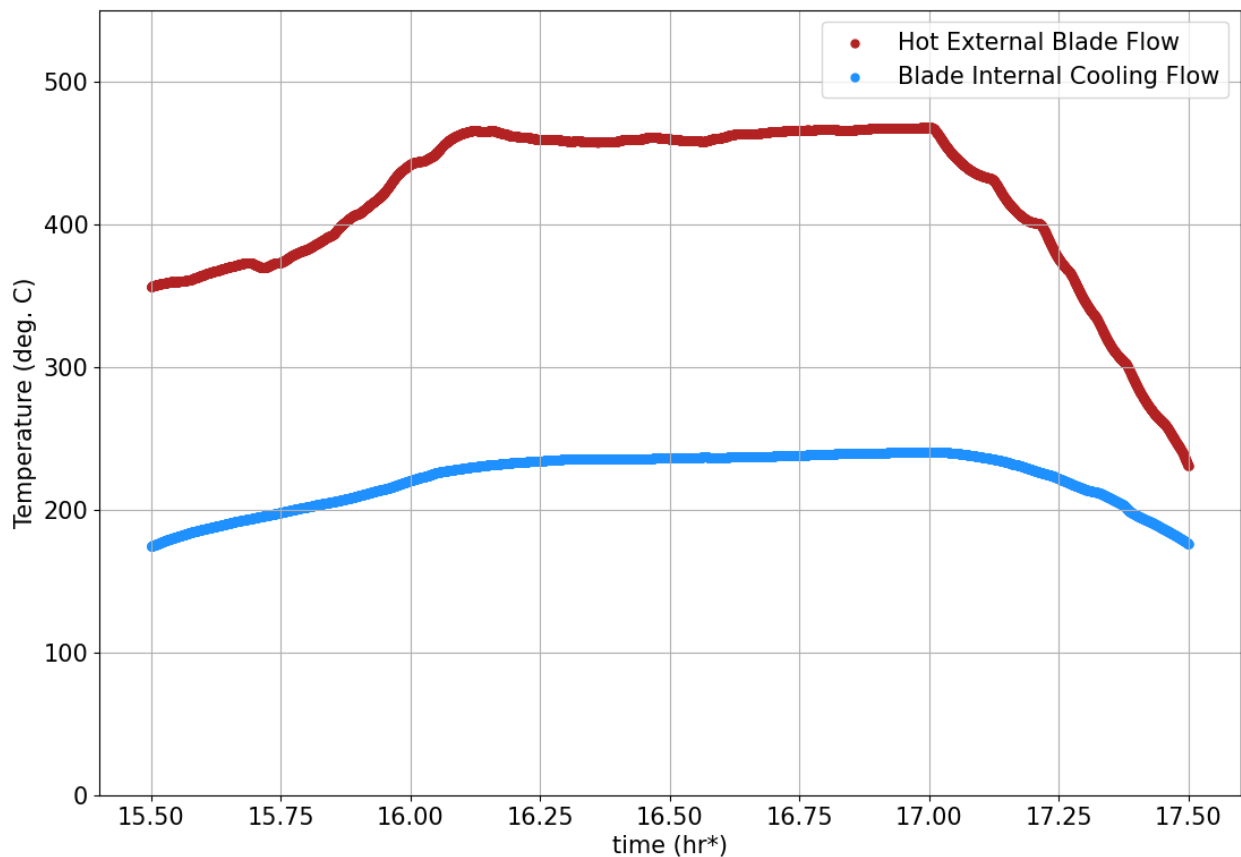


Figure 6. Temperature profile during main part of testing for hot external blade flow and blade internal cooling flow. Time is expressed as hours into the day on the test day.

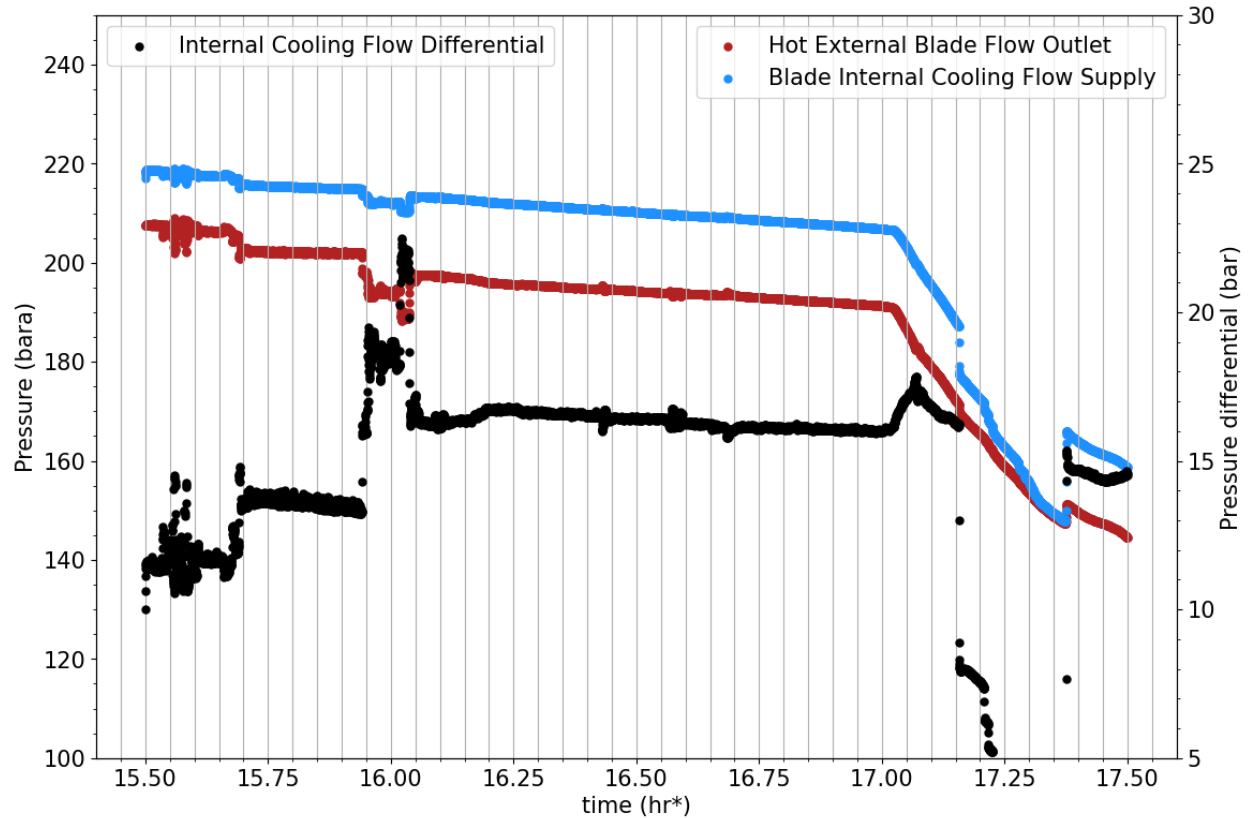


Figure 7. Pressure profile during main part of testing for hot external blade flow and blade internal cooling flow supply. The internal cooling flow differential represents the calculated difference between these values that enables the appropriate cooling flow rate through the blade. Time is expressed as hours into the day on the test day.

Flow rates are calculated for the hot external blade flow through an orifice flow meter (ORF-374), while flow rates through the blade are calculated with the 1-D thermal and hydraulic network. The hydraulic network for the blade internals includes major and minor pressure losses through the blade passages and pin-fin array, and a discharge coefficient of 0.85 for the exit cooling holes based on a velocity head ratio over 100 [11]. The respective flow rates are summarized in Table 1.

Table 1. Flow rate data during predicted time of maximum blade metal temperature. The uncertainty in hot external blade flow is due to the fundamental uncertainty in discharge coefficient for the orifice plate (ASME MFC-14M-2003), the uncertainty in blade cooling flow is an estimate based on assumptions made for discharge coefficients and pressure loss correlations used.

Flow Rate	Calculation	Value (kg/s)	Bias Uncertainty
Hot external blade flow	Orifice flow meter (ORF-374)	1.605	±0.8%
Blade internal cooling flow	1-D hydraulic flow network	0.032	±10% (estimated)

The UCTS were post-processed with a normalized temperature history chart and X-ray diffractometry analysis completed by LG-Tech Link Global. The max temperatures, with an

expected random error of measurement with standard deviation ($\pm 3.3^\circ\text{C}$) at each sensor location are seen in Figure 8.

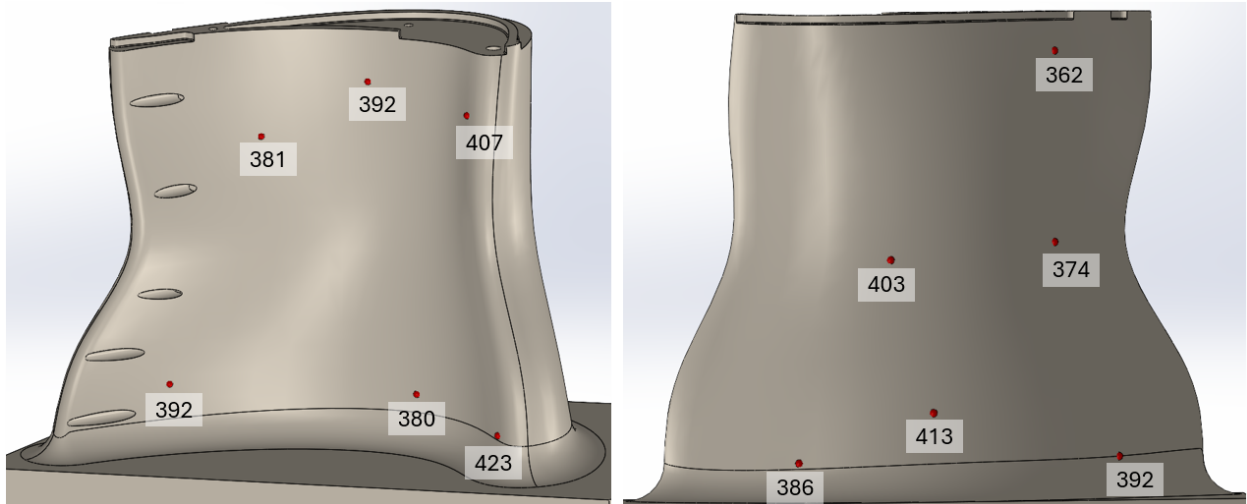


Figure 8. Max metal temperatures post-processed from UCTS for six pressure (Left) and suction (Right) surface locations visualized through the red spheres.

In comparison with the hot external blade flow temperature of 468°C at the assumed point in time, the cooling flow reduced the metal temperature locally between 45°C and 106°C below the external gas path temperature. The cooling flow assumed temperature is 240°C , the average between the closest temperature measurements of 224°C and 257°C equidistant at the inlet and exit ports to the test section case.

ANALYTICAL METHOD AND COMPARISON

The analytical method to predict blade wall temperatures used CFD for external blade heat transfer conditions, and the 1-D thermal and hydraulic network for the internal heat transfer conditions. ANSYS CFX [12] was implemented for simulation of the external blade domain with a SST turbulence model and CO_2 real gas tabulated fluid properties from the NIST REFPROP database [13]. The domain included the upstream and downstream tubular flow sections, and all pertinent flow features around the blade including the upstream and downstream flow conditioning plates. The central blade is assigned a roughness of 125 Ra and the surrounding walls a roughness of 500 Ra as they were not ground as the central blade was. A total pressure and total temperature inlet with a mass flow rate outlet target were set according to the measured hot external flow conditions, those corresponding to the 17 hr. mark in Figure 6 and Figure 7. Point source flow conditions were assigned at the locations of tip cooling ejection holes to accurately resolve downstream effects on the blade external heat load. Additionally, the blade surface was given a heat transfer coefficient boundary condition of $6317 \text{ W/m}^2\text{-K}$ and source temperature of 257°C . The values are the average total thermal resistance across the blade wall and internal cooling flow and the average internal cooling flow temperature, respectively. Mesh settings were iterated to adhere to a wall y-plus value between 30 and 300 for the blade surface. The domain around the blade, and contours of the wall adjacent temperature and wall heat transfer coefficient are seen in Figure 9.

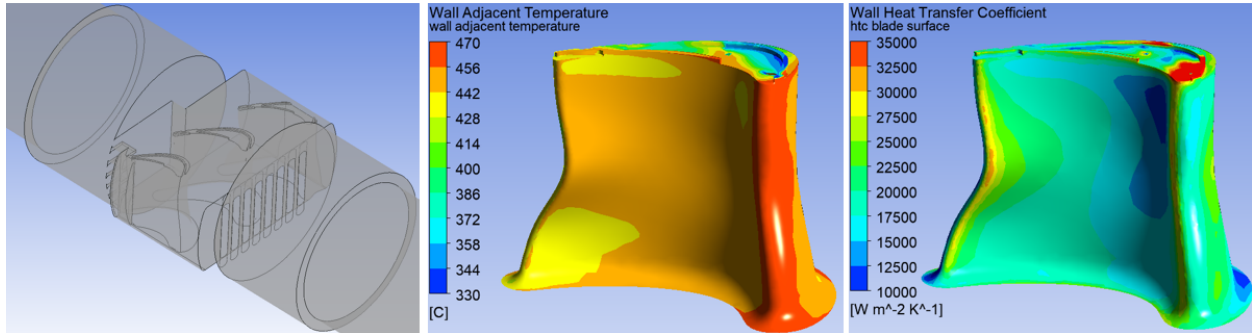


Figure 9. From L to R: Fluid domain simulated; wall adjacent temperature along the blade pressure surface; wall heat transfer coefficient along the pressure surface.

The purpose of the 1-D thermal and hydraulic network is to generate the heat transfer boundary conditions for the ANSYS 3-D thermal model, namely heat transfer coefficients and source temperatures for each blade internal geometry region. Boundary conditions for the 1-D model included the cooling flow internal feed pressure and temperature at the 17 hr. mark along with the external hot flow downstream static pressure. As described in the previous work [2], the 1-D network calculates HTC's using the Chupp correlation for leading edge impingement and Metzger for the trailing edge pin fin array to agree with experimental work [4,6]. Gnielinski correlations are used for the mid-section ribbed serpentine passages, with a Nusselt number enhancement ratio of 3.0 to match previous data in the Reynolds number regime between 100,000 and 200,000 [5]. In addition to the previously discussed discharge coefficient assumptions, further hydraulic calculations are done for friction factor ratios through the ribbed passages and pressure drop through the pin fin section to predict with greater accuracy the flow potential across cooling discharge holes. Another key component is the prediction of internal flow temperature increase through the passages. The heat rejection magnitude is calculated by assuming an average blade surface temperature and calculating the total thermal resistance across the blade walls and internal cooling flow. The internal heat transfer boundary conditions assigned for the fully resolved internal geometry of the 3-D ANSYS thermal model is seen in Figure 10. The external boundary conditions are applied to both the central blade and surrounding platform and neighboring blade surfaces using the exported wall adjacent temperature and wall heat transfer coefficient in Figure 9.

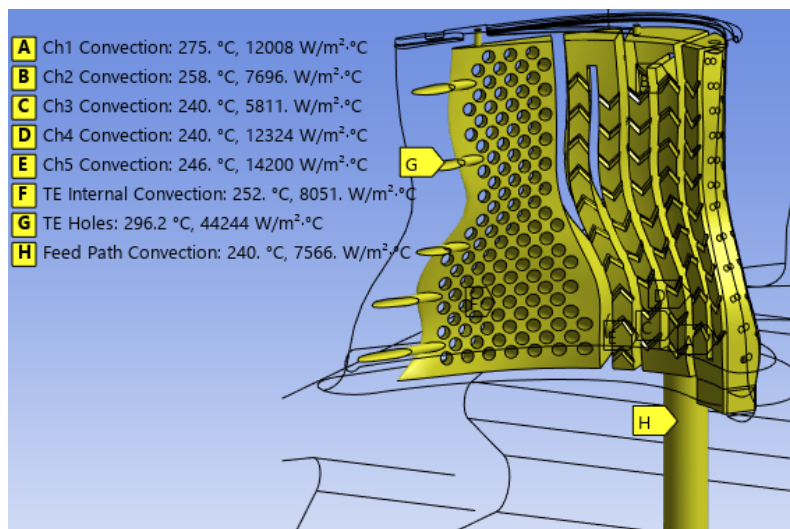


Figure 10. Internal flow heat transfer boundary conditions for the S1B in the ANSYS thermal FE model. Each boundary condition is applied to the individual surfaces it governs.

The 3-D thermal model employs tabulated thermal conductivity properties for the Inconel 718 blade material. The resolved temperature profile with all internal and external heat transfer conditions applied is seen in Figure 11. The nodal results for the temperature profile are exported and the nodal temperature with closest proximity to each UCTS sensor installation coordinate is collected for comparison to the UCTS post-processed temperature, enumerated in Table 2.

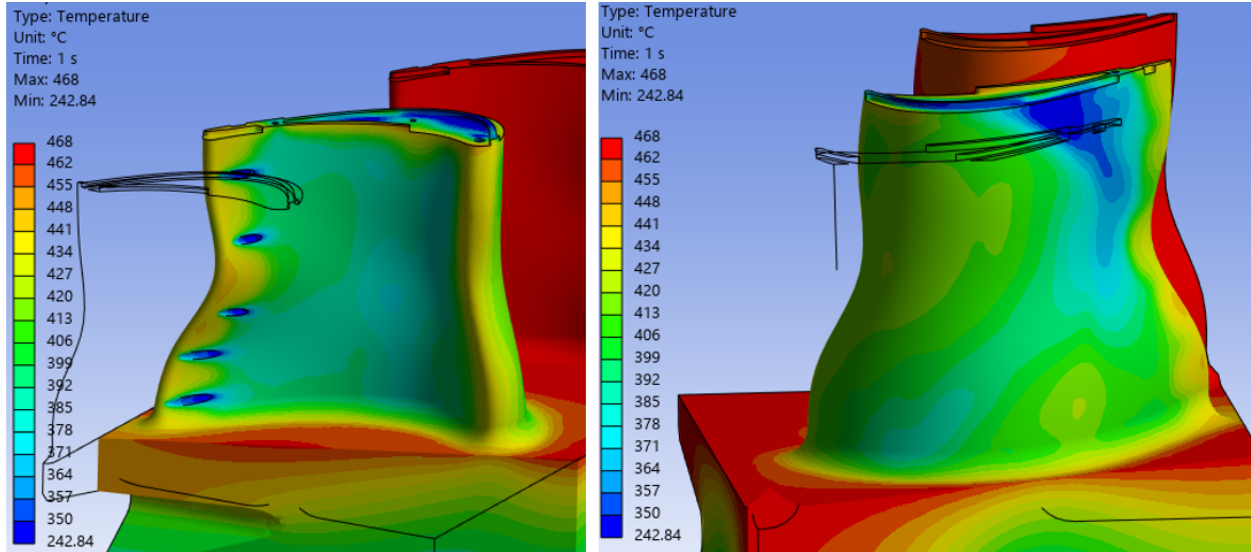


Figure 11. Left: Resolved temperature profile of the pressure surface. Right: resolved temperature profile of the suction surface.

Table 2. Comparison of UCTS temperature and 3-D thermal model predicted temperature. PS stands for pressure surface, SS for suction surface.

Location	UCTS temp. (°C)	Predicted temp. (°C)	Difference (°C)
PS1	423	422	-1
PS2	407	413	+6
PS3	381	386	+5
PS4	392	386	-6
PS5	392	395	+3
PS6	380	384	+4
SS1	392	403	+11
SS2	413	409	-4
SS3	386	389	+3
SS4	374	368	-6
SS5	362	358	-4
SS6	403	410	+7

The average absolute temperature difference between the predicted temperature profile with the analysis methodology and the UCTS test data is 5.0°C. To understand which regions of the blade saw relative higher differences, Figure 12 illustrates the difference in predicted temperature profile relative to the test data in Figure 8. It should be noted as stated previously that the UCTS test values have an expected random error of measurement with standard deviation ($\pm 3.3^\circ\text{C}$).

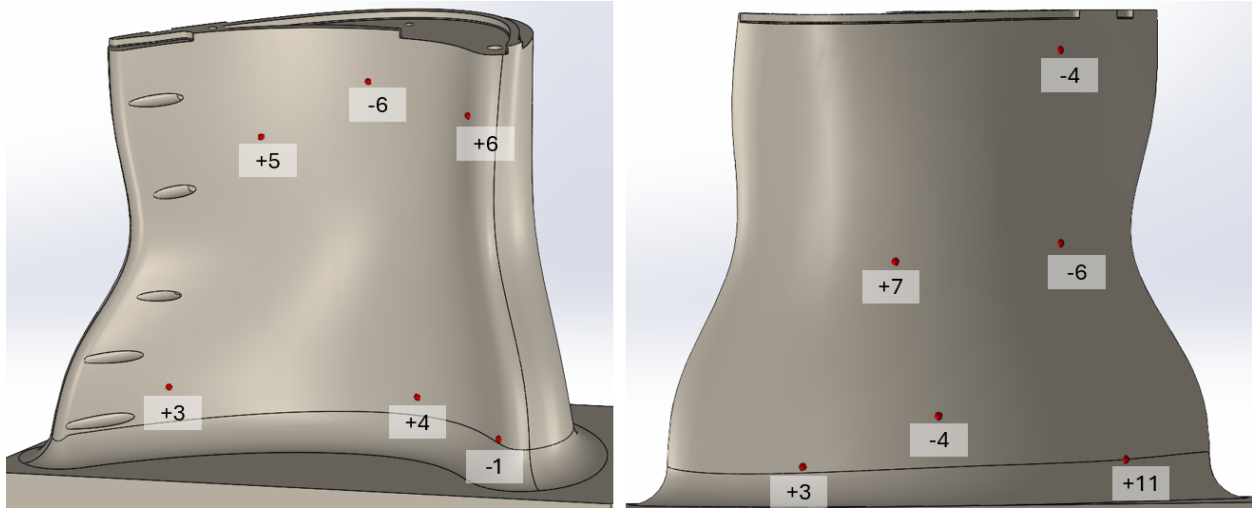


Figure 12. At each UCTS location, the value displayed is the difference between the predicted metal temperature using the analysis methodology and the UCTS local value.

CONCLUSION

A test campaign was completed to resolve the temperature profile of a stationary S1B cascade with internal cooling in a sCO_2 environment with temperatures up to 468°C and pressures of approximately 200 bar. The temperature profile used the UCTS instrumentation method to find the maximum temperature experienced during the test at 12 total locations spanning the pressure and suction surfaces. These results were used to compare to the predictions from a 3-D FE blade temperature prediction employing heat transfer surface conditions emanating from external flow CFD and an internal 1-D thermal and hydraulic network model. The 1-D thermal model predicts heat transfer coefficients for a Reynolds number range for sCO_2 typically extending far higher than typical air breathing engine cooling. The prediction methodology had previously been used for the full turbine conditions with TIT of 1150°C to predict the blade life and associated cooling flow requirements. Due to the relationship between creep strength and metal temperature, it is vital to have close agreement with the prediction methodology for it to be useful in the conceptual and detailed design phases of turbine design. Based on the comparison between UCTS temperature and predictions at the same location having an average absolute deviation of 5.0°C over 12 locations with a maximum of 11°C , the analysis methodology is judged to be of high value for predicting cooling flow requirements and blade life early in a detailed design phase. The use of 1-D thermal networks for resolving internal cooling can save considerable time during design iteration when compared to the use of 3-D CFD. In the same vein, while the methodology contained in this paper used 3-D CFD for the external heat transfer conditions, the early stages of the design phase could leverage empirical correlation based external heat load predictions. Future work should focus on testing rotating internally cooled blades for direct-fired sCO_2 turbine application, as well as UCTS instrumentation for nozzles that would employ film cooling and require further comparison with prediction methodologies of air-breathing engine legacy.

ACKNOWLEDGEMENT

This material is based upon work supported by the U.S. Department of Energy under Award Number DE-FE0031929.

DISCLAIMER

This report was prepared as an account of work sponsored by an agency of the United States Government. Neither the United States Government nor any agency thereof, nor any of their employees, makes any warranty, expressed or implied, or assumes any legal liability or responsibility for the accuracy, completeness, or usefulness of any information, apparatus, product, or process disclosed, or represents that its use would not infringe privately owned rights. Reference herein to any specific commercial product, process, or service by trade name, trademark, manufacturer, or otherwise does not necessarily constitute or imply its endorsement, recommendation, or favoring by the United States Government or any agency thereof. The views and opinions of authors expressed herein do not necessarily state or reflect those of the United States Government or any agency thereof.

REFERENCES

1. Allam, R.J., Fetvedt, J.E., Forrest, B.A., Freed, D.A (2014). "The Oxy-Fuel, Supercritical CO₂ Allam Cycle: New Cycle Developments to Produce Even Lower-Cost Electricity from Fossil Fuels without Atmospheric Emissions". Proceedings of the ASME Turbo Expo 2014: Turbomachinery Technical Conference and Exposition. GT2014-26952.
2. Marshall, M., Anguiano, M., Bensmiller, J., Replogle, C., Kerr, T., Klaerner, J., Moore, J.J. (2025). "Detailed Design and Cost Estimation of a 300 MWe Oxy-Fuel sCO₂ Turbine". Proceedings of the ASME Turbo Expo 2025: Turbomachinery Technical Conference and Exposition. GT2025-154107.
3. Tuite, L., Braun, J., Paniagua, G. (2024). "Optimization of a High Pressure Turbine Blade and Sector-Based Annular Rig Design for Supercritical CO₂ Power Cycle Representative Testing". ASME J Eng Gas Turbines Power., 146(6):061017. GTP-23-1463.
4. Richardson, J., Wardell, R., Fernandez, E., Kapat, J.S. (2023). "Experimental and Computational Heat Transfer Study of sCO₂ Single-jet Impingement". Proceedings of the ASME Turbo Expo 2023: Turbomachinery Technical Conference and Exposition. GT2023-102544.
5. Marshall, M., Anguiano, M., Moore, J.J. (2024). "Heat Transfer Experiments of Ribbed, Serpentine Cooling Passages with Supercritical CO₂". Proceedings of the 8th International Supercritical CO₂ Power Cycles Symposium. Paper #67.
6. Wardell, R., Richardson, J., Otto, M., Smith, M., Fernandez, E., Kapat, J. (2023). "An Experimental Investigation of Heat Transfer for Supercritical Carbon Dioxide Cooling in a Staggered Pin Fin Array". Proceedings of the ASME Turbo Expo 2023: Turbomachinery Technical Conference and Exposition. GT2023-103263.
7. Haynes International (2023). "Haynes 282 Alloy". H-3173F. URL: <https://haynesintl.com/wp-content/uploads/2023/09/282-brochure.pdf>
8. Thomas, A., Ginzursky, Ed. (2025) "Uniform Crystal Temperature Sensor Technology and Support Services: Principle of Operation". LG Tech-Link Global. URL: <https://lgtechlink.com/principle-of-operation/>.

9. Brown, J, DeVoe, J, & Ginzursky, L. "The Challenges of Uniform Crystal Temperature Sensor (UCTS) Application in Turbomachinery." Proceedings of the ASME Turbo Expo 2013: Turbine Technical Conference and Exposition. Volume 3C: Heat Transfer. San Antonio, Texas, USA. June 3–7, 2013.
10. Ho, K, Liu, J, Urwiller, C, Konan, SM, & Aguilar, B. "Conjugate Heat Transfer Analysis of a Cooled Turbine Blade Using Frozen Rotor Approach." Proceedings of the ASME Turbo Expo 2015: Turbine Technical Conference and Exposition. Volume 5A: Heat Transfer. Montreal, Quebec, Canada. June 15–19, 2015.
11. Han, J.C., Dutta, S., Ekkad, S. (2013). *Gas Turbine Heat Transfer and Cooling Technology, 2nd Edition*. Section 4.2.10. CRC Press.
12. ANSYS® CFX, Release 19.2.
13. Lemmon, E.W., Bell, I.H., Huber, M.L., McLinden, M.O. NIST Standard Reference Database 23: Reference Fluid Thermodynamic and Transport Properties-REFPROP, Version 9.1, National Institute of Standards and Technology, Standard Reference Data Program, Gaithersburg, 2013.